

Climatology of horizontal winds in the lower and middle atmosphere over an equatorial station – Thiruvananthapuram

Geetha Ramkumar¹ and Veena Suresh Babu²

¹Space Physics Laboratory, Vikram Sarabhai Space Centre, Thiruvananthapuram 695 022, India

²All Saints' College, Thiruvananthapuram 695 008, India

The climatology of prevailing horizontal winds in the 0–98 km region over an equatorial station Thiruvananthapuram is presented here. The climatology of horizontal winds is derived by making use of monthly mean zonal and meridional winds obtained from four decades of balloon flights (1970–2010), three decades of rocket flights (1971–1993, 2002–2007) and one decade of SKiYMET meteor wind radar (2004–2014) observations. The observed climatology is compared with the global scale wave model (GSWM-09), and similarities and differences are discussed. Seasonal trends in the horizontal winds and features specific to the equatorial region are also discussed.

Keywords: Climatology, equatorial station, horizontal winds, middle atmosphere.

THE dynamics of equatorial middle atmosphere is of great interest due to the presence of long-period waves, tides, planetary waves and gravity waves which are comparable in magnitude to that of the prevailing winds. Middle atmospheric dynamics and its variability remained far from being understood mainly owing to lack of observations, especially in the 30–60 km height region. Over the global atmosphere, the equatorial and low-latitude middle atmosphere show distinctly different behaviour, due to large solar isolation, relatively less Coriolis force, quasi biannual oscillation (QBO) and semi-annual oscillations (SAO) present in the zonal wind^{1–4}. For validation purposes and for estimation of derived parameters in linear models, there is a need for prevailing wind parameters in the middle atmosphere. There exist well-established models such as COSPAR international reference atmosphere (CIRA)⁵ and Horizontal Wind Model (HWM93) (ref. 6), but they do not represent the wind systems in this height regions of middle atmosphere very well, especially in the equatorial region. Therefore, updated models mainly based on radar and satellite observations have been developed and recently, models of the semi-diurnal and diurnal tidal parameters (Global Empirical Wind Model (GEWM))⁷ augment them. However, GEWM is

restricted to the mesopause region, and can only serve as a model for that height region. Comprehensive models of the middle atmosphere must incorporate data from a variety of instruments having different measurement techniques covering different regions of the atmosphere.

There are several existing climatologies for the stratosphere, compiled using data from the US National Meteorological Centre (NMC)^{8,9}, which provided four-year climatology for the northern and southern winter. CIRA^{10,11} is a collection of monthly mean wind and temperature fields and its vertical extent has the credit of giving the first climatology of zonal mean for the mesosphere of both the hemispheres, but it cannot compete with the dataset used by Randel *et al.*¹².

There are models which provide a glimpse of the mesospheric circulation. But these models are not valid in the tropics, since the geostrophic approximation fails there¹³ and also the observational database used from low latitude is less compared to those from mid- and high-latitudes. Portnyagin *et al.*¹⁴ have given a detailed review of mesospheric and lower thermospheric models and discussed the main reasons for the differences among them.

Being a transition zone between the stratosphere and thermosphere, the mesosphere–lower thermosphere (MLT) region is of interest. This is a region where upward-propagating disturbances from the lower atmosphere, such as gravity waves and tides, reach their maximum amplitudes and break, depositing momentum and energy into the large-scale flow. This is also a region where signals of global atmospheric change such as the effects of increases in CO₂ are significantly greater than that in the troposphere and stratosphere^{15–17}. Over the past two decades, a number of numerical models have been developed to explore various phenomena in the MLT region. Although these models are able to reproduce many of the observed features of the MLT region, they do not represent a broad spectrum of geophysical variability.

The general circulation pattern over mid- and high-latitude mesosphere is fairly well-understood through various observational techniques and theoretical studies^{18–21}, but poorly understood over low latitudes. There are reports on the long-term changes in thermospheric neutral winds over Arecibo based on over three decades

*For correspondence. (e-mail: veenasbabu@gmail.com)

of Fabry–Perot observations²². Only a few studies have been carried out in equatorial and low latitudes with limited dataset using VHF radar^{23,24}, rocket soundings²⁵, MF radar^{26,27} and meteor radar²⁸ observations. Early observations of mean winds at low latitudes and their comparison with other ground-based, model and satellite techniques were confined to limited dataset spanning four years²⁴. There are reports about the climatological features in the low-latitude mesospheric horizontal winds using data collected from Indian MST radar²⁹. Sasi and Sengupta³⁰ developed an empirical reference atmospheric model (temperature, pressure, density) applicable to 0–15°N lat. in the 0–80 km height region at the Indian equatorial zone, making use of balloon and rocket observations over a period of 16 years from Thiruvananthapuram. The zonal wind observations in the 70–80 km height range over the Indian region provided by rocketsonde HRDI/UARS, and MST radar during 1977–2010 showed a decreasing trend of 2 m/s/year changing from strong eastward winds to weak westward winds in recent years³¹. Pramitha *et al.*³² also reported climatological monthly mean contours of temperature, zonal wind and meridional wind obtained over Gadanki region combining a variety of instruments.

Climatology and statistics play an essential role in understanding the meteorological processes. Statistical information and detailed studies of wave motions in the upper atmospheric levels are useful as they provide clues of association with large-scale weather phenomena. The equatorial middle atmospheric region being populated with interesting dynamical features, is a critical region which couples the upper and lower atmosphere. The present study delineates the climatological characteristics of mean winds in the entire middle atmospheric region. We have used a new dataset to bring out vertical structure of climatological mean horizontal winds (both zonal and meridional) in the middle atmospheric region over an equatorial location.

Data and method of analysis

In the present study, data on zonal and meridional winds obtained from balloon-borne measurements for a period of four decades (1970 January–2010 December) have been used in order to derive climatology of mean winds in the 0–25 km height region. Using about three decades January 1971–December 1993 and November 2002–November 2007 of rocketsonde (both M-100 and RH-200 rockets) measured zonal and meridional wind data, climatological pattern of horizontal winds in the 26–65 km region has been derived. In the 66–80 km region over the present location, wind information is available only from M-100 rocket observations during the period 1971–1993. A minimum of three profiles is available in the height region of 66–80 km for each month during the period of

observations, though they are less compared to those in the height regions below and above. The climatological structure of zonal and meridional winds in the 82–98 km height region is derived from the meteor wind radar observations during 10 years starting from 2004 June to 2014 May. Figure 1 *a–c* shows the number of observations used for the present study. Figure 1 *a* represents the number of observations of zonal wind (u) and meridional wind (v) in the 0–25 km region during 1970–2010 from balloon-borne radiosonde data. Balloon flights are conducted regularly at 1400 h at the present observational site. A minimum of four observations is available in a month. Figure 1 *b* shows the number of observations of u and v , from rocketsonde during 1971–2007 in the 26–80 km region. M100 rocket flights are conducted mostly at fixed timings around 2000 h and RH 200 rocket flights are conducted at 1130 h from Thiruvananthapuram. On an average, 3–4 rocketsonde observations are available in a month. Campaign mode of balloon and rocket flights were conducted during diurnal cycles for tidal oscillation studies, which were also included for monthly mean winds in addition to the regular observations at fixed timings. Figure 1 *c* represents the number of observations of u and v in the 82–98 km height region derived from SKiYMET meteor wind radar data during the period 2004–2014. In the case of radar data, hourly u , v values are averaged to have daily mean u and v and then averaged to get monthly mean u , v values. On an average, 28 days

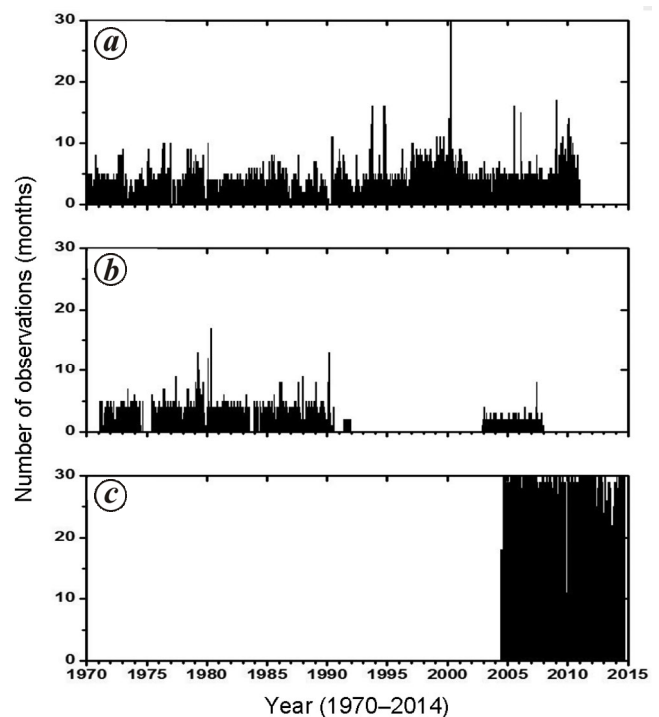


Figure 1. Histogram of zonal wind and meridional wind observations using (a) radiosonde flights, (b) rocketsonde and (c) SKiYMET meteor wind radar.

of observations are available for each month. Since balloon and rocket flights are conducted at different timings giving one shot information and radar gives hourly values of winds, making use of data collected from radar at the same time as that of balloon or rocket will drastically reduce the volume of the data. The monthly averaged wind data of radar from diurnally averaged data when compared with those derived from daily data averaged over few hours were found to be within the standard deviation itself. The main limitation of the data used in the present study is that they are collected by using different experimental techniques from different regions of the atmosphere at different timings; hence the errors involved in the measurements also differ. Since the focus of the present study is on the climatology of winds in the 0–98 km height region, which cannot be made with data from single observational technique, it was decided to make use of all the available databases at the study location to get monthly mean winds. Also, more the data, better the climatological picture.

High-altitude balloons carrying radiosondes and radar targets were used for measuring altitude profiles of wind, temperature, humidity and pressure in the 0–35 km altitude region. Since all balloon measurements do not give data up to 35 km, we restricted the wind data from radiosondes to 25 km only. The accuracies of the radiosonde wind measurements are $1\text{--}2\text{ ms}^{-1}$ and 5° for wind speed and wind direction respectively, for wind speeds above 25 ms^{-1} . RH-200 is an indigenously developed two-stage rocket, which uses chaff as a payload to measure winds in the 25–65 km altitude region. Devarajan *et al.*³³ have shown that the standard errors involved in the RH 200 chaff-measured wind components are $2\text{--}2.7\text{ ms}^{-1}$ in the 20–50 km region and 3.8 ms^{-1} above 50 km region. The Soviet M100 rocket system is a two-stage, solid-fuel rocket motor with a payload to measure temperature, pressure and wind at 2 km height resolution. The maximum error in wind measurements the 66–80 km height region from M100 rocket is $\sim 6\text{ m s}^{-1}$. In the 82–98 km region, we have used the SKiYMET meteor wind radar observations to derive zonal and meridional winds. A general description of the SKiYMET meteor wind radar can be found in Hocking *et al.*³⁴. Radial velocity can be measured with an accuracy of 5% or more, and temperature with an accuracy of about 10 K or more^{35,36}. The zonal and meridional wind data are averaged on a monthly basis over the entire period and then monthly average for each calendar month of all years averaged in order to obtain climatological mean database for each calendar month. The long-term trend in the climatological mean of each calendar month is removed using trend-removal technique in order to get better results for each calendar month (January–December) in the entire height region of 0–98 km.

Global scale wave model (GSWM) is a numerical model for planetary waves and solar tides in the earth's

atmosphere from 0 to about 125 km, developed at the High Altitude Observatory (HAO), National Centre for Atmospheric Research (NCAR)³⁷. The standard GSWM background atmosphere is available along with tidal results which account for realistic tidal forcing due to ozone and water vapour, and the effects of empirical background climatologies of zonal mean temperature, neutral density, zonal wind and ozone concentration, as well as wave dissipation. In the present study the observed climatology of prevailing zonal winds in the 0–98 km region at 8.5°N is compared with the zonally averaged zonal winds at 10°N from the GSWM-2009 model.

Results and discussion

Height structure of zonal and meridional winds

The climatological mean zonal and meridional winds during each calendar month derived from four decades of balloon flights, three decades of rocket flights and a decade of SKiYMET meteor wind radar observations are combined together to get the height structure of horizontal winds in the 0–98 km region during January–December. Figure 2a and b depicts the height structure of zonal and meridional winds along with standard errors in the 0–98 km region during January–December. The observed height structures of mean zonal winds from the present observations (shown in black colour along with error bars) are compared with GSWM-2009 model corresponding to 10°N lat. (shown in red colour), which is the latest model available for prevailing winds in the entire height region of interest close to the observational site. It is to be noted that the GSWM-2009 model provides zonal mean zonal winds.

During winter months of January and February, the observed and model profiles follow the same trend with much closer values, while in November and December, observed values are slightly more than model values. In January and February, the zonal wind values are westward below 30 km with amplitudes less than 10 ms^{-1} and reach maximum westward amplitude of $\sim 30\text{ ms}^{-1}$ at the stratopause. Then zonal winds change eastward in the mesospheric region with maximum eastward amplitude of 30 ms^{-1} around 70 km and again change westward in the upper mesospheric–lower thermospheric region. During March and April below 30 km altitude though the zonal wind is relatively weak, it changes direction abruptly generating a shear around 20 km. In the upper mesosphere region, the westward wind reaches a maximum of $\sim 60\text{ ms}^{-1}$ around 80 km during April and then decreases with increase in height. It is clearly seen that the peak of westward zonal wind descends below 40 km and eastward peak broadens during January–April. From April onwards, small-scale disturbances start appearing throughout the lower atmospheric region and continue up to November.

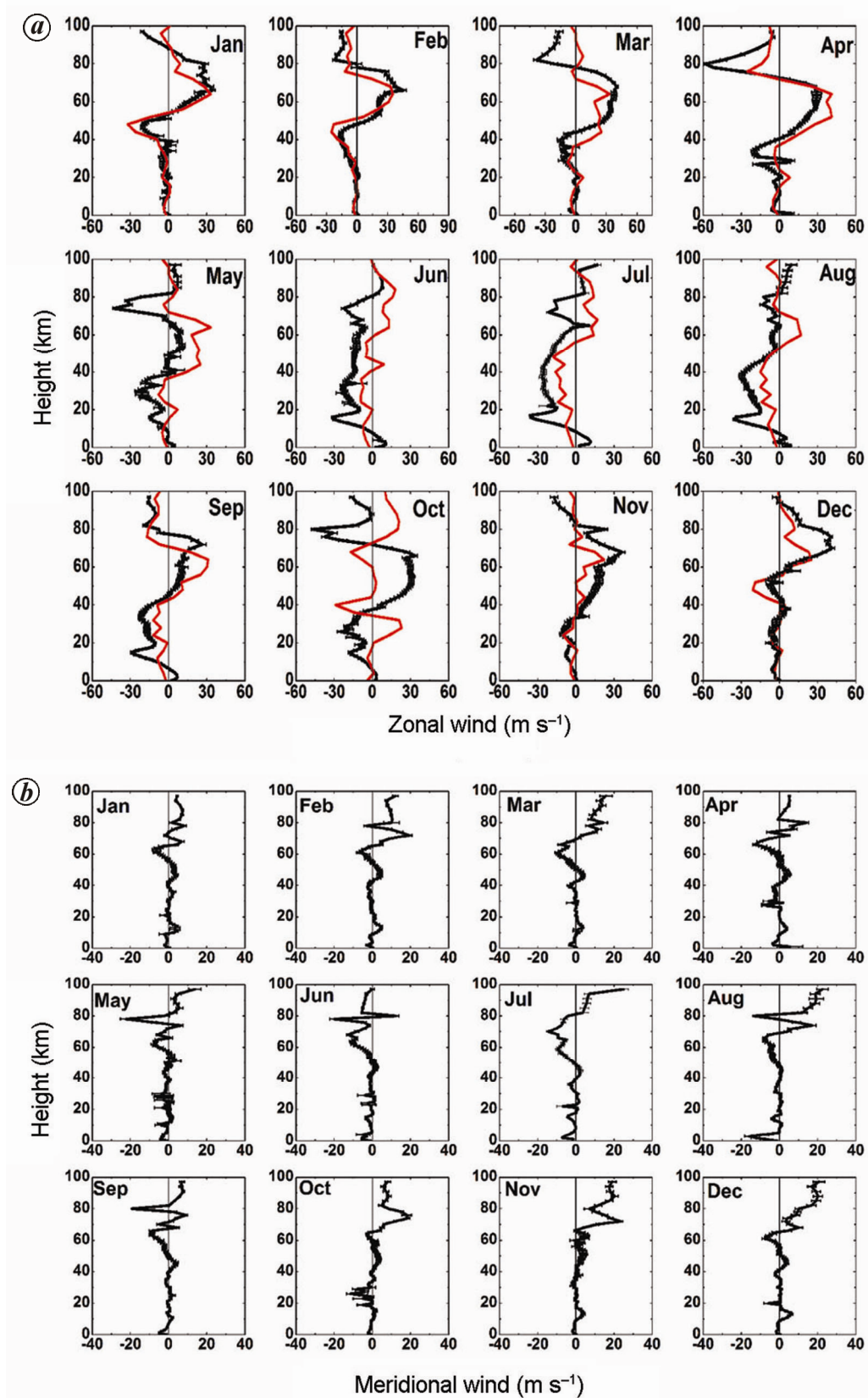


Figure 2. *a*, Height profiles of observed climatological mean zonal winds in the 0–98 km height region (black line) along with error bars, compared with GSWM-09 model (red line). *b*, Height profiles of observed climatological mean meridional winds in the 0–98 km region during January–December.

The short-scale perturbations in the observed profiles in the middle atmosphere, especially during May–October are present in the model profiles; they are the specific features in the tropical region during monsoon period. But the observational values deviate from the model values in amplitude and direction at certain height regions during these months. In May, the eastward winds in the lower mesosphere and westward winds in the upper mesosphere are weakened and start reversing their direction.

During June–August, it is observed that below 80 km the zonal wind is generally westward and above 80 km it is eastward. Though the general trend with short-scale perturbations is reproduced in the model profiles in the mesospheric region, it deviates in amplitude and direction, especially during June and July. A strong easterly jet is present near the tropopause during the summer monsoon months (June–September) and maximum amplitude of 45 ms^{-1} is observed in July. The presence of tropical easterly jet (TEJ) near the tropopause with large amplitude during June–September, which is the specific feature at the observational site, is not reproduced in the GSWM model. It is obvious that the zonal mean zonal wind will not represent these features as it is restricted to the Indian region only and while doing zonal mean, it will not be standing out. The sub-daily variation of TEJ³⁸ and the characteristics of TEJ in different phases of monsoon³⁷ are already reported for tropical latitudes³⁸. Monsoon low-level jet with maximum amplitude of 10 m/s during monsoon months at this location in the height region 0–5 km is also a distinct feature in the observed profiles, which is absent in the model profiles.

During the southwest summer monsoon months of June–September, the observed values are slightly larger than model values over the equatorial station where TEJ and prevailing monsoon circulation are present during this period. Reports by India Meteorological Department (IMD) show that during the monsoon months of June–August, westward zonal flows dominate both in the stratosphere and mesosphere with a maximum mean speed of 30 ms^{-1} at 38 km level in August (Meteorological Monograph, Climatology/No. 20/2000, 1998). During other months, the mesosphere is dominated by eastward zonal flow and the stratosphere is dominated by westward zonal flow with varying heights in the level of transition between the two flows. This level of transition appears to be forced upwards as the monsoon season advances.

During September and October, the TEJ weakens and the westward wind changes eastward above 40 km; above 70 km it changes westwards again. The zonal winds are found to have maximum amplitude of 33 ms^{-1} near 60 km in October. The model and the observed zonal wind profiles show entirely different structure, especially in the stratospheric–mesospheric region in October. This peculiar feature over the present location could be due to the prevailing monsoon circulation. During November and

December, the observed values are found to be slightly higher than the model values above 60 km, but the trend remains generally the same and the large-scale structures are regained as in the case of January and February. Generally, the model profiles during winter and vernal equinox seasons follow the same trend as that of the observed profiles, and show different structure during summer season and October.

Figure 2b depicts the climatology of meridional winds in the 0–98 km region for January–December. The meridional wind magnitudes are generally smaller compared to those of zonal winds. During January–April in the tropospheric and stratospheric region, a weak northward wind is observed with a small peak of 6 ms^{-1} around 10 km and 50 km. Above stratopause in the 50–60 km region it changes direction from northward to southward and then again changes northward in the lower thermospheric heights. In the 60–80 km region, northward wind reaches a maximum of 20 ms^{-1} at 70 km in February and above that, the amplitude decreases with height. During March–May, a maximum northward amplitude of $\sim 5 \text{ ms}^{-1}$ is observed near 50 km and a maximum southward amplitude of 10 ms^{-1} observed near 60 km. Above 80 km, the winds remain northward with amplitudes of 15 ms^{-1} in March and May. During May–September, meridional winds are found to be southward in the lower mesospheric heights with maximum amplitude of 30 ms^{-1} . During May and June as well as August and September in the 60–98 km region, the winds change from southward to northward and again southward indicating large shear. In all other months, above 80 km the wind is generally northward with larger amplitudes, especially during March, July–August, November and December. Presence of monsoon low-level jet is also seen in meridional winds in the 0–5 km height region.

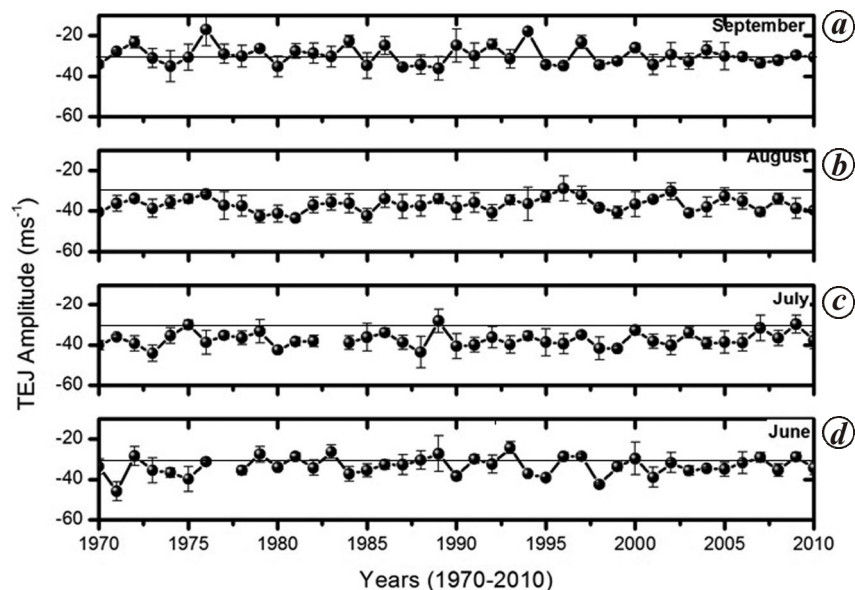
Table 1 shows the prominent characteristics in the height structure of observed zonal and meridional winds in the 0–98 km region. It describes the maximum amplitudes of the climatological zonal (eastward and westward) and meridional (northward and southward) winds along with their standard errors for each calendar month. The heights at which these values become maximum and minimum are shown in brackets.

Tropical easterly jet at Thiruvananthapuram over four decades

From Figure 2a, it can be clearly seen that the prominent feature of zonal wind peculiar to this location and which is not reproduced in the model, is the presence of strong easterly jet around tropopause region during summer monsoon season. Since four decades of data are available, it is interesting to look into the variation of TEJ strength at the present location over the entire data length. Figure 3a–d shows the variation in amplitude of TEJ along with

Table 1. Maximum amplitudes of the climatological mean zonal (eastward and westward) and meridional (northward and southward) winds along with their standard errors for each calendar month. The heights at which these values become maximum and minimum are shown in brackets

Month	Zonal wind		Standard error (zonal wind)		Meridional wind		Standard error (meridional wind)	
	Eastward maximum (ms ⁻¹)	Westward maximum (ms ⁻¹)	Minimum (ms ⁻¹)	Maximum (ms ⁻¹)	Northward maximum (ms ⁻¹)	Southward maximum (ms ⁻¹)	Minimum (ms ⁻¹)	Maximum (ms ⁻¹)
January	34.5 (66 km)	-20.63 (97 km)	0.15 (1 km)	4.59 (51 km)	8.2 (78 km)	-6.47 (63 km)	0.18 (1 km)	2.66 (13 km)
February	45.7 (66 km)	-21.86 (82 km)	0.12 (1 km)	5.59 (78 km)	19.3 (72 km)	-7.03 (78 km)	0.12 (1 km)	4.74 (80 km)
March	46.2 (68 km)	-38.58 (82 km)	0.21 (1 km)	7.56 (36 km)	15.76 (97 km)	-9.55 (61 km)	0.16 (1 km)	3.23 (97 km)
April	30 (66 km)	-58.2 (71 km)	0.037 (78 km)	3.95 (65 km)	14 (80 km)	-13.1 (66 km)	0.15 (82 km)	6.71 (1 km)
May	10.78 (55 km)	-42.7 (74 km)	0.17 (1 km)	6.22 (41 km)	13.75 (97 km)	-22.3 (78 km)	0.17 (1 km)	4.93 (28 km)
June	10.77 (2 km)	-30.93 (16 km)	0.18 (1 km)	8.74 (34 km)	12.5 (80 km)	-19.9 (78 km)	0.09 (1 km)	3.71 (29 km)
July	16.97 (94 km)	-35.92 (16 km)	0.21 (1 km)	6.54 (21 km)	24.98 (94 km)	-14.5 (68 km)	0.14 (1 km)	3.18 (21 km)
August	9.29 (97 km)	-35.99 (15 km)	0.18 (1 km)	4.49 (82 km)	22.48 (97 km)	-15.95 (3 km)	0.11 (1 km)	3.75 (91 km)
September	26.4 (69 km)	-29.18 (15 km)	0.3 (1 km)	3.00 (74 km)	8.9 (76 km)	-19.3 (80 km)	0.19 (1 km)	1.75 (78 km)
October	33.5 (66 km)	-46.4 (80 km)	0.18 (1 km)	5 (23 km)	18.6 (74 km)	-11.49 (26 km)	0.01 (80 km)	5.06 (23 km)
November	36.3 (68 km)	-17.13 (97 km)	0.09 (31 km)	3.07 (72 km)	23.4 (72 km)	-2.01 (2 km)	0.09 (1 km)	2.77 (80 km)
December	41.3 (70 km)	-8.7 (20 km)	0.14 (1 km)	6.37 (58 km)	20.6 (97 km)	-7.75 (61 km)	0.09 (1 km)	3.03 (97 km)

**Figure 3.** Time series of amplitudes of tropical easterly jet (TEJ) for (a) June, (b) July, (c) August and (d) September during 1970–2010.

standard deviation during June, July, August and September respectively, over the study period of four decades. The amplitude is found to be maximum during June–August and is weakened towards September. Maximum TEJ amplitude of more than 45 ms^{-1} is observed during June 1971, July 1973, July 1980, July 1988 and June 1998. The line drawn at 30 ms^{-1} is to follow the WMO definition of TEJ. During August, the amplitude of TEJ varies more or less between 30 and 40 ms^{-1} . In September, 60% of the TEJ amplitude is found to be relatively small, with values between 30 and 35 ms^{-1} . From the analysis of the height of occurrence of maximum amplitude of TEJ, it is found that maximum amplitude occurred mostly around 15–16 km. But occasionally, the height of maximum amplitude reached 17 km during June 1994, 2006 and 2008. Large year-to-year variability in TEJ seen from seventies to nineties is absent in recent decades and the amplitude on an average has shown varying trends during the four decades. Since several studies have already been done or are being done on TEJ^{38–40}, a detailed discussion on TEJ characteristics is not provided here.

Time height section of climatological mean horizontal winds over the equatorial station

To have a three-dimensional picture of wind structure covering all seasons, the time height behaviour of climatological mean zonal and meridional winds in the 0–98 km region over the equatorial station is presented in Figure 4a and c respectively. Figure 4b shows the time height behaviour of zonal wind values provided by GSWM-2009 model.

From Figure 4a, the presence of TEJ is clearly seen around the tropopause region during June–September with maximum strength during June and August. In the 25–40 km height region, zonal winds are predominantly westward with a maximum amplitude of 25 ms^{-1} during July. In the 40–80 km region, zonal winds are found to be predominantly eastward with maximum amplitude of 20 ms^{-1} during winter and equinoctial seasons. During summer months, amplitudes were as low as 5 ms^{-1} . The presence of stratopause SAO in zonal wind is clearly seen in Figure 4a. In the 80–98 km height region during winter season, zonal winds are found to be weak westward and are of the order of 5 ms^{-1} . During equinoctial months (March and April; September and October), zonal winds become strong with a maximum amplitude of 25 ms^{-1} in the 85 km region. During June–September, winds are weak eastward and amplitudes are of the order of 5 ms^{-1} . The features seen in the observed zonal winds are reproduced in the model winds shown in Figure 4b, except the presence of TEJ and descending easterlies in the mesosphere during March–May. There are reports about the climatological monthly mean structure of zonal and

meridional winds obtained over Gadanki region using a variety of instruments³², which agree well with our present observations over Thiruvananthapuram.

Generally, the meridional amplitude values are less (Figure 4c) compared to those of zonal winds. The meridional wind is found to be weak below 50 km with amplitudes of $\pm 5 \text{ ms}^{-1}$ for all seasons. Around 60 km, the meridional wind becomes southward with an amplitude of 15 ms^{-1} . In the 70–80 km region, the meridional winds are mostly northward during winter and equinoxes, and southward during summer months. In the 80–98 km region, winds are predominantly northward throughout the year.

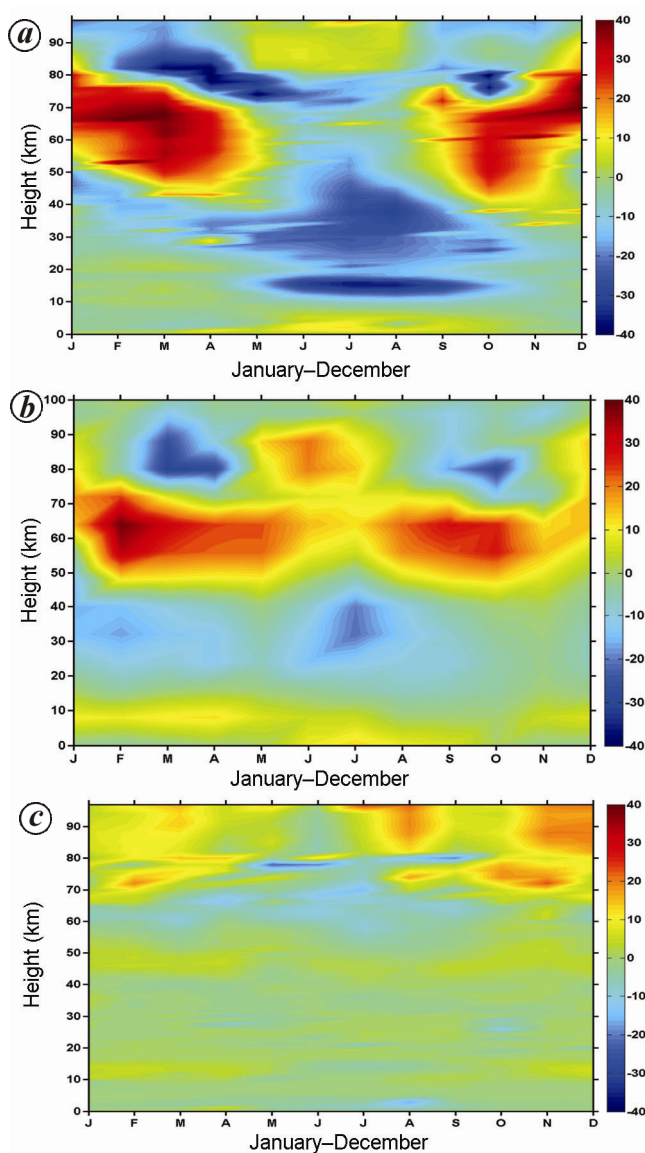


Figure 4. Time–height section of (a) observed climatological mean zonal winds over the present observational site, (b) GSWM-2009 derived zonal winds at 10°N and (c) observed climatological mean meridional winds in the 0–98 km region over the present observational site.

Summary

Neutral atmospheric wind measurements from the surface to ~100 km height region are necessary, especially to derive atmospheric models appropriate to different locations. The present study establishes the detailed climatology of horizontal winds in the 0–98 km height region over an equatorial station Thiruvananthapuram. The equatorial region being significantly different from mid- and high-latitudes, studies on the dynamics of this region, especially that of middle atmospheric region, are crucial for understanding dynamical coupling between different regions of the atmosphere. This information is specifically required as it forms an essential input for design of sounding rockets, satellite launch vehicles and for aerodynamic studies. Observational studies conducted from the present site, spread over four decades of radiosonde, three decades of rocket and nearly a decade of ground-based radar measurements could bring out several unique features of mean horizontal winds during various seasons. The vertical structure of the equatorial middle atmospheric winds could be reasonably well understood from the climatology of mean wind pattern over the station. Comparison of the observed height structure of mean zonal winds in the 0–98 km region with GSWM-2009 model values shows that the observed features are mostly reproduced, except during June–October, which could be due to the peculiar characteristics of winds during monsoon months.

During the monsoon months of June–August, westward zonal wind dominates both in the stratosphere and mesosphere. During other months, the mesosphere is dominated by eastward zonal winds and stratosphere is dominated by westward zonal flow with varying heights in the level of transition between these two flows. This level of transition appears to be forced upwards as the monsoon season advances. The strong TEJ during June–September with maximum amplitude of 45 ms^{-1} during June and July is one of the most important features specific to this location, which is not captured by the GSWM-2009 model. This is because the model uses zonal mean zonal wind and is restricted to the Indian region; so while doing zonal mean, features will be smoothed out. Monsoon low-level jet is also found to be a prominent feature over the present location in the 0–5 km altitude region, with core strength around 10 ms^{-1} and axis lying in the southeast direction. Thus, the present study establishes the climatology of horizontal winds in the 0–98 km region using balloon, rocket and radar observations, bringing out unique features over the equatorial station.

1. Reed, R. J., The present status of 26-month oscillation. *Bull. Am. Meteorol. Soc.*, 1965, **46**, 374–387.
2. Reed, R. J., The quasi biennial oscillation of the atmosphere between 30 and 50 km over Ascension Island. *J. Atmos. Sci.*, 1965, **22**, 331–333.

3. Hirota, I., Equatorial waves in the upper stratosphere and mesosphere in relation to the semi-annual oscillation of the zonal wind. *J. Atmos. Sci.*, 1978, **35**, 714–722.
4. Andrews, D. G., Holton, J. R. and Leovy, C. B., *Middle Atmosphere Dynamics*, Academic Press, San Diego, Calif., 1987, p. 489.
5. Fleming, E. L., Chandra, S., Barnett, J. J. and Corney, M., Zonal mean temperature, pressure, zonal wind and geopotential height as function of latitude. *Adv. Space Res.*, 1990, **10**(12), 11–59; doi: 10.1016/0273-1177(90)90386-E.
6. Hedin, A. E., Fleming, E. L. and Manson, A. H., Empirical wind model for the upper, middle and lower atmosphere, *J. Atmos. Terr. Phys.*, 1996, **58**, 1421–1447; doi: 10.1016/0021-9169(95)00122-0.
7. Portnyagin, Y., A review of mesospheric and lower thermosphere models. *Adv. Space Res.*, 2006, **38**(11), 2452–2460; doi: 10.1016/j.asr.2006.04.030.
8. Geller, M. A., Wu, M. F. and Gelman, M. E., Troposphere stratosphere (surface ~55 km) monthly winter general circulation statistics for the northern hemisphere – four year averages. *J. Atmos. Sci.*, 1983, **40**, 1344–1352.
9. Mechoso, C. R., Hartmann, D. L. and Farrara, J., Climatology and interannual variability of wave mean-flow interaction in the southern hemisphere. *J. Atmos. Sci.*, 1985, **42**, 2189–2206.
10. Barnett, J. J. and Corney, M., Temperature data from satellites. In *Handbook Middle Atmosphere Programme* (eds Labitzke, K. and Barnett, J. J.), 1985, vol. 16, pp. 3–11.
11. Barnett, J. J. and Corney, M., Middle atmosphere reference model derived from satellite data. In *Handbook Middle Atmosphere Programme* (eds Labitzke, K. and Barnett, J. J.), 1985, vol. 16, pp. 47–85.
12. Randel, W. *et al.*, The SPARC intercomparison of middle-atmosphere climatologies. *J. Climate*, 2004, **17**, 986–1003.
13. Hirota, I., Hirooka, T. and Shitani, M., Upper stratospheric circulations in the two hemispheres observed by satellites, *Q.J.R. Meteorol. Soc.*, 1983, **109**, 443–454; doi:10.1002/qj.49710946102.
14. Portnyagin, Y. *et al.*, Mesosphere/lower thermosphere prevailing wind model. *Adv. Space Res.*, 2004, **34**, 1755–1762; doi: 10.1016/j.asr.2003.04.058.
15. Berger, U. and Dameris, M., Cooling of the upper atmosphere due to CO₂ increases: a model study. *Ann. Geophys.*, 1993, **11**, 809–819.
16. Akmaev, R. A. and Fomichev, V. I., A model estimate of cooling in the mesosphere and lower thermosphere due to the CO₂ increase over the last 3–4 decades. *Geophys. Res. Lett.*, 2000, **27**(14), 2113–2116.
17. Akmaev, R. A., Fomichev, V. I., Gavrilov, N. M. and Shved, G. M., Simulation of the zonal mean climatology of the middle atmosphere with a three-dimensional spectral model for solistice and equinox conditions. *J. Atmos. Terr. Phys.*, 1992, **54**, 119–128.
18. Meek, C. E. and Manson, A. H., Combination of primrose lake ROCOB winds (20–60 km) and Saskatoon MF radar winds (60–110 km) – 1978–1983. *J. Atmos. Terr. Phys.*, 1985, **47**, 477–487.
19. Nakamura, T., Tsuda, T., Yamamoto, Fukao, S. and Sato, K., Characteristics of gravity waves in the mesosphere observed with the middle and upper atmosphere radar 1. Momentum flux, *J. Geophys. Res.*, 1993, **98**(D5), 8999–8910.
20. Manson, A. H. *et al.*, Mean winds of the upper middle atmosphere (~70–110 km) from the global radar network: comparisons with CIRA 72, and new rocket and satellite data. *Adv. Space Res.*, 1987, **7**(10), 143–153.
21. Middleton, H. R., Mitchell, N. J. and Muller, H. G., Mean winds of the mesosphere and lower thermosphere at 52°N in the period 1988–2000. *Ann. Geophys.*, 2002, **20**, 81–91.
22. Brum, C. G. M., Craig, A. T., Fentzke, J. T. and Robles, E., Pedrina Terra dos Santos and Gonzalez, S. A., Long-term changes in the thermospheric neutral winds over Arecibo: climatology based on over three decades of Fabry-Perot observations. *J. Geophys. Res., Space Physics*, 2012, **117**, 1–16; doi:10.1029/2011JA016458.

23. Hitchman, M. H. *et al.*, Mean winds in the tropical stratosphere and mesosphere during January 1993, March 1994 and August 1994. *J. Geophys. Res.*, 1997, **102**, 26033–26052.
24. Ratnam, M. V., Rao, D. N., Rao, T. N., Thulasiraman, S., Nee, J. B., Gurubaran, S. and Rajaram, R., Mean winds observed with Indian MST radar over tropical mesosphere and comparison with various techniques. *Ann. Geophys.*, 2001, **19**, 1027–1038.
25. Chakravarty, S. C., Datta, J. and Revankar, C. P., Climatology of long-period oscillations in the equatorial middle atmosphere over Thumba, India. *Curr. Sci.*, 1992, **63**, 33–42.
26. Vincent, R. A., Long period motions in the equatorial middle atmosphere. *J. Atmos. Terr. Phys.*, 1993, **55**, 1067–1080.
27. Rajaram, R. and Gurubaran, S., Seasonal variabilities of low-latitude mesospheric winds. *Ann. Geophys.*, 1998, **16**, 197–204.
28. Reddi, C. R. and Ramkumar, G., The annual and semi-annual wind fields in low latitudes. *J. Atmos. Terr. Phys.*, 1997, **59**, 487–495.
29. Kishore Kumar, G. *et al.*, Low-latitude mesospheric mean winds observed by Gadanki mesosphere–stratosphere–troposphere (MST) radar and comparison with rocket, High Resolution Doppler Imager (HRDI), and MF radar measurements and HWM93. *J. Geophys. Res.*, 2008, **113**, D19117; doi: 10.1029/2008JD009862.
30. Sasi, M. N. and Sen Gupta, K., A reference atmosphere for the Indian equatorial zone from surface to 80 km. *Sci. Rep.*, SPL:SR:006:85, 1986.
31. Venkat Ratnam, M., Kishore Kumar, G., Venkateswara Rao, N., Krishna Murthy, B. V., Lastovicka, J. and Qian, L., Evidence of long-term change in zonal wind in the tropical lower mesosphere: observations and model simulations. *Geophys. Res. Lett.*, 2013, **40**, 1–5; doi: 10.1002/grl.50158.
32. Pramitha, M., Venkat Ratnam, M., Taori, A., Krishna Murthy, B. V., Pallamraju, D. and Vijaya Bhaskar Rao, S., Evidence for tropospheric windshear excitation of high-phase-speed gravity waves reaching the mesosphere using the ray-tracing technique. *Atmos. Chem. Phys.*, 2015, **15**, 2709–2721.
33. Devarajan, M., Parameswaran, P. R., Reddy, C. A. and Reddy, C. R., Accuracy of stratospheric wind measurements using chaff releases from RH-200 rockets. *Indian J. Radio Space Phys.*, 1984, **13**, 48–55.
34. Hocking, W. K., Fuller, B. and Vandeppeer, B., Real time determination of meteor-related parameters utilizing modern digital technology. *J. Atmos. Sol. Terr. Phys.*, 2001, **63**, 155–169.
35. Deepa, V., Ramkumar, G., Antonita, T. M., Kumar, K. K. and Sasi, M. N., Vertical propagation characteristics and seasonal variability of tidal wind oscillations in the MLT region over Trivandrum (8N, 77E): first results from SKiYMET meteor radar. *Ann. Geophys.*, 2006, **24**, 1–13.
36. Kumar, K. K., Ramkumar, G. and Shelbi, S. T., Initial results from SKiYMET meteor radar at Thumba (8.5°N, 77°E), 1. Comparison of wind measurements with MF spaced antenna radar system. *Radio Sci.*, 2007, **42**, RS6008; doi: 10.1029/2006RS003551.
37. GSWM model 2009, developed by Maura Hagan, hagan@ucar.edu
38. Venkat Ratnam, M. *et al.*, Sub-daily variations observed in Tropical Easterly Jet (TEJ) streams. *J. Atmos. Sol. Terr. Phys.*, 2011, **73**, 731–740.
39. Roja Raman, M., Jagannadha Rao, V. V. M., Venkat Ratnam, M., Rajeevan, M., Rao, S. V. B., Narayana Rao, D. and Prabhakara Rao, N., Characteristics of the Tropical Easterly Jet: long-term trends and their features during active and break monsoon phases. *J. Geophys. Res.*, 2009, **114**, D19105; doi: 10.1029/2009-JD012065.
40. Venkat Ratnam, M., Krishna Murthy, B. V. and Jayaraman, A., Is the trend in TEJ reversing over the Indian subcontinent? *Geophys. Res. Lett.*, 2013, **40**, 1–4; doi: 10.1002/grl.50519.

ACKNOWLEDGEMENTS. This work was supported by the Department of Space, Government of India. V.S.B. thanks the Indian Space Research Organization for financial support through a research fellowship. We also thank Maura Hagan, National Center for Atmospheric Research, Boulder for providing GSWM09 data; the Meteorology Facility and Advanced Technology Vehicle and Sounding Rockets Project of Vikram Sarabhai Space Centre (VSSC), Thiruvananthapuram for providing necessary data for the present study, and the engineers and scientists of Space Physics Laboratory, VSSC for support in collecting a good database from meteor Wind Radar.

Received 19 February 2015; revised accepted 14 March 2016

doi: 10.18520/cs/v111/i3/500-508